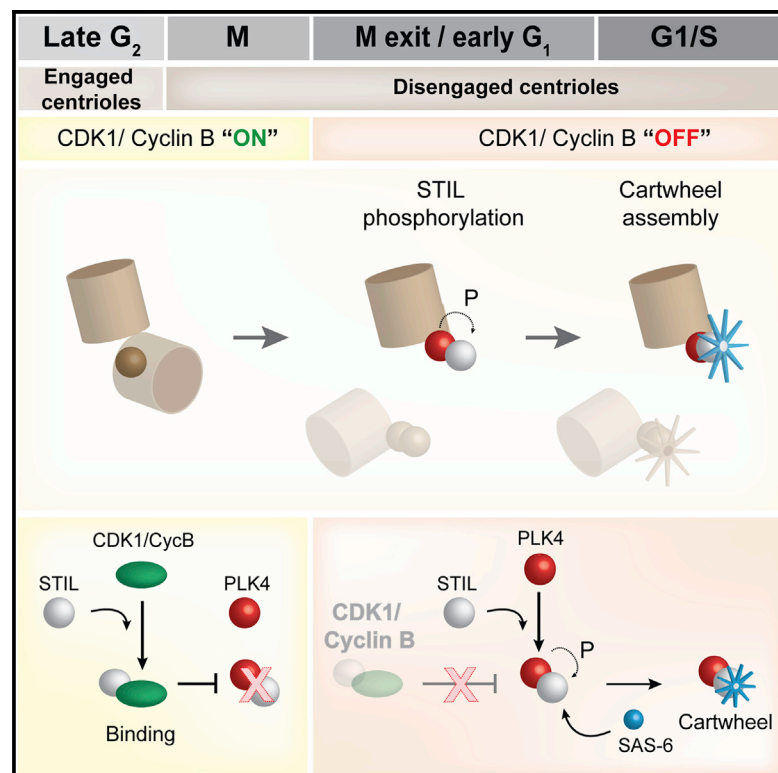


CDK1 Prevents Unscheduled PLK4-STIL Complex Assembly in Centriole Biogenesis

Graphical Abstract



Authors

Sihem Zitouni, Maria E. Francia,
Filipe Leal, ..., Thierry Lorca,
Mariana Lince-Faria,
Mónica Bettencourt-Dias

Correspondence

zsihem@igc.gulbenkian.pt (S.Z.),
mfrancia@igc.gulbenkian.pt (M.E.F.),
mdias@igc.gulbenkian.pt (M.B.-D.)

In Brief

Zitouni, Francia et al. explore the mechanisms coupling the cell cycle to centrosome biogenesis, and show that in mitosis, CDK1 competes with PLK4, the trigger of centriole biogenesis, for binding to its substrate STIL. PLK4 binding and phosphorylation of STIL occurs only upon CDK1 activity drop at mitotic exit, leading to centriole biogenesis onset.

Highlights

- PLK4 activity is needed in G₁ for centriole biogenesis
- PLK4 binds its substrate STIL upon inactivation of CDK1-CyclinB
- CDK1-CyclinB binds to STIL in mitosis through the same domain to which PLK4 binds
- CDK1-CyclinB prevents PLK4 from binding and phosphorylating STIL



CDK1 Prevents Unscheduled PLK4-STIL Complex Assembly in Centriole Biogenesis

Sihem Zitouni,^{1,8,*} Maria E. Francia,^{1,8,*} Filipe Leal,¹ Susana Montenegro Gouveia,¹ Catarina Nabais,¹ Paulo Duarte,¹ Samuel Gilberto,^{1,10} Daniela Brito,¹ Tyler Moyer,⁵ Steffi Kandels-Lewis,^{2,3} Midori Ohta,⁴ Daiju Kitagawa,⁴ Andrew J. Holland,⁵ Eric Karsenti,^{2,6} Thierry Lorca,⁷ Mariana Lince-Faria,^{1,9} and Mónica Bettencourt-Dias^{1,9,*}

¹Instituto Gulbenkian de Ciência, Rua da Quinta Grande 6, Oeiras 2780-156, Portugal

²Directors' Research, European Molecular Biology Laboratory, Meyerhofstrasse 1, Heidelberg 69117, Germany

³Structural and Computational Biology, European Molecular Biology Laboratory, Meyerhofstrasse 1, Heidelberg 69117, Germany

⁴Center for Frontier Research, National Institute of Genetics, Yata 1111, Mishima, Shizuoka 411-8540, Japan

⁵Department of Molecular Biology and Genetics, Johns Hopkins University School of Medicine, 725 North Wolfe Street, Baltimore, MD 21205, USA

⁶Ecole Normale Supérieure, Institut de Biologie de l'ENS (IBENS), Inserm U1024, and CNRS UMR 8197, 46 Rue d'Ulm, Paris 75005, France

⁷Centre de Recherche de Biochimie Macromoléculaire, CNRS UMR 5237, 1919 Route de Mende, Montpellier 34293, France

⁸Co-first author

⁹Co-senior author

¹⁰Present address: Department of Biology, Institute of Biochemistry, Swiss Federal Institute of Technology, 8093 Zurich, Switzerland

*Correspondence: zsihem@igc.gulbenkian.pt (S.Z.), mfrancia@igc.gulbenkian.pt (M.E.F.), mdias@igc.gulbenkian.pt (M.B.-D.)

<http://dx.doi.org/10.1016/j.cub.2016.03.055>

SUMMARY

Centrioles are essential for the assembly of both centrosomes and cilia. Centriole biogenesis occurs once and only once per cell cycle and is temporally coordinated with cell-cycle progression, ensuring the formation of the right number of centrioles at the right time. The formation of new daughter centrioles is guided by a pre-existing, mother centriole. The proximity between mother and daughter centrioles was proposed to restrict new centriole formation until they separate beyond a critical distance. Paradoxically, mother and daughter centrioles overcome this distance in early mitosis, at a time when triggers for centriole biogenesis Polo-like kinase 4 (PLK4) and its substrate STIL are abundant. Here we show that in mitosis, the mitotic kinase CDK1-CyclinB binds STIL and prevents formation of the PLK4-STIL complex and STIL phosphorylation by PLK4, thus inhibiting untimely onset of centriole biogenesis. After CDK1-CyclinB inactivation upon mitotic exit, PLK4 can bind and phosphorylate STIL in G1, allowing pro-centriole assembly in the subsequent S phase. Our work shows that complementary mechanisms, such as mother-daughter centriole proximity and CDK1-CyclinB interaction with centriolar components, ensure that centriole biogenesis occurs once and only once per cell cycle, raising parallels to the cell-cycle regulation of DNA replication and centromere formation.

INTRODUCTION

Centrosomes are the main microtubule-organizing centers (MTOCs) of mammalian cells [1], composed of two centrioles.

These are surrounded by the pericentriolar material, which nucleates microtubules and organizes the cytoskeleton. Centrioles can also nucleate the ciliary axoneme. Centriole number is highly controlled in cells; abnormalities can lead to defects in spindle and cilium assembly [1]. A new (daughter) centriole normally forms in physical proximity to a pre-existing (mother) centriole; this occurs once and only once per cell cycle (centriole-guided assembly). When no pre-existing centrioles are found in a cell, centrioles can also form “de novo,” and in this case they form in random numbers [1]. Interestingly, the timing of centriole biogenesis is conserved in both; new centrioles only form in S phase [2].

Both centriole-guided and de novo biogenesis are dependent on and initiated by Polo-like kinase 4 (PLK4) [3–5]. In the case of centriole-guided biogenesis, PLK4 is recruited to the proximal end of the mother centriole, determining the place of biogenesis [6]. PLK4 binds and phosphorylates STIL (SCL/TAL1/SAS5/Ana2), recruiting it to the centriole [7–11]. Phosphorylated STIL in turn brings SAS6 to the centrioles to form the centriole cartwheel [7, 8], the first visible structure in centriole assembly that helps in defining the centriolar 9-fold symmetry [12]. Overexpression or stabilization of PLK4, STIL, or SAS6 leads to supernumerary centrioles, whereas their individual depletion blocks centriole duplication [3, 12].

Centriole biogenesis is tightly coupled to cell-cycle progression. The formation of the cartwheel is detectable early in S phase, concomitant with the start of DNA replication [1, 13]. Paradoxically, PLK4, STIL, and SAS6 are present at the centrosome in mid-G1 up until the end of mitosis [9, 14–16]. The physical proximity between mother and daughter centriole is thought to prevent formation of yet another daughter centriole in S, G2, and mitosis [1, 17]. However, already in a natural or arrested prophase and prometaphase, mother and daughter centriole reach a critical distance from each other shown to be permissive for centriole reduplication, yet they do not reduplicate at that stage [18–20]. Moreover, it has been shown in both *Drosophila* and *Xenopus* egg extracts that although PLK4 can induce de novo

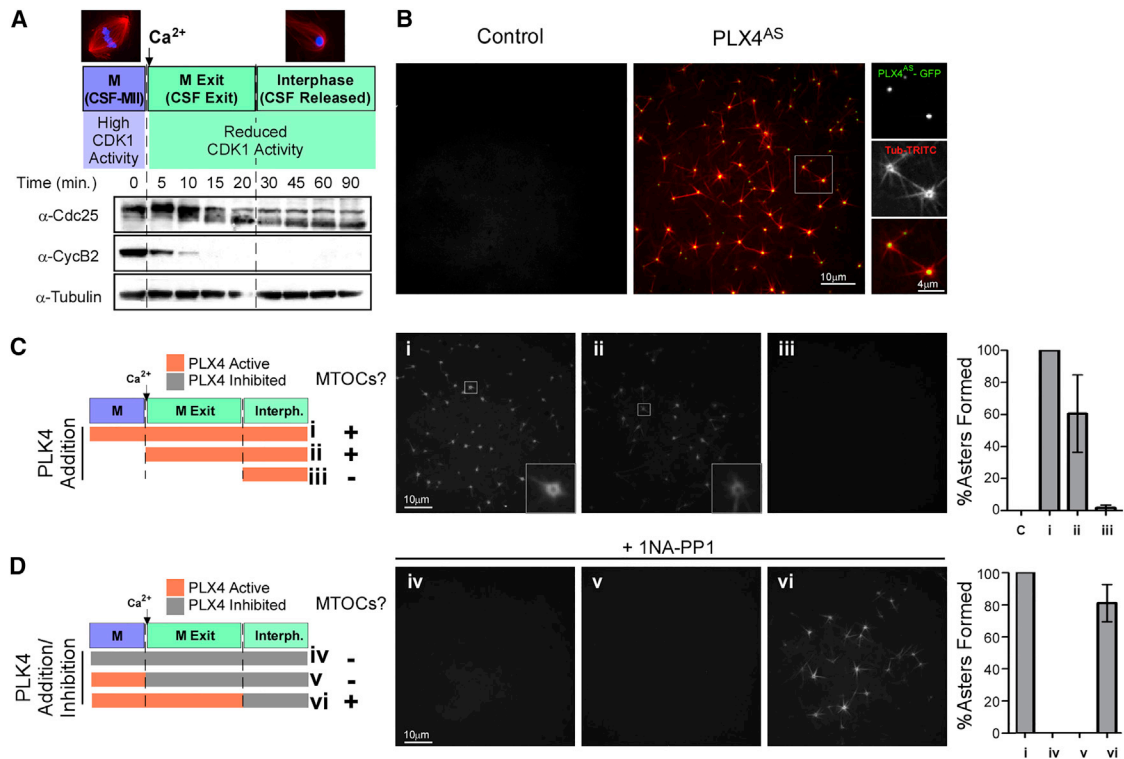


Figure 1. PLX4 Induces De Novo Aster Formation Early after M Phase Release in *Xenopus* Egg Extracts

(A) Cell-cycle profiling of *Xenopus* M phase extracts released with Ca^{2+} . Western blotting (WB) shows the kinetics of Cdc25 downshift and Cyclin B2 degradation leading to reduced CDK1 activity.

(B) GFP-PLX4^{AS} induces MTOC formation in M phase-released extracts. CSF extract was incubated with 0.65 μM GFP-PLX4^{AS} (green) and TRITC-tubulin (red). Insets represent enlarged asters of the corresponding box in the image. See Figures S1 and S2C for the generation and characterization of Shokat alleles (see also Movies S1 and S2).

(C) Cell-cycle-dependent effect of PLX4. rPLX4 was added at different time points, (i) 10 min before release (addition of Ca^{2+}), (ii) concomitant with release, and (iii) 20 min after release, in order to check when PLX4 activity is needed to form MTOCs (TRITC-tubulin). C, negative control (buffer). Insets are an enlarged aster of the corresponding boxes in each respective representative image.

(D) Inhibition of PLX4^{AS} using 1-NA-PP1 at different stages. PLX4^{AS} was added 10 min before Ca^{2+} . 1-NA-PP1 was then added at different time points to the extracts: (iv) time zero (concomitant with the addition of PLX4^{AS}), (v) at the time of Ca^{2+} release, and (vi) 20 min after Ca^{2+} release.

Panels of MTOCs formed in the extract under each condition, stained with TRITC-tubulin, are shown. Asters were counted in ten images for each condition and normalized to the number of asters observed in the positive control extracts (i); (n = 3; bars represent average \pm SD).

MTOC formation upon meiosis exit, it cannot do it in meiosis-arrested eggs or extracts [21, 22]. Together, these facts suggest the existence of additional levels of regulation during high CDK1-CyclinB activity phases, such as mitosis and meiosis.

Here we explore the mechanism that couples cell-cycle progression to the first molecular events in centriole biogenesis: PLK4-STIL complex formation and STIL phosphorylation. We show that CDK1-CyclinB prevents precocious PLK4-STIL complex assembly and STIL phosphorylation by PLK4, through direct binding to STIL. Upon mitotic exit and consequent CDK1-CyclinB degradation, PLK4 can bind and phosphorylate STIL, which recruits SAS6.

RESULTS

We first asked when the activity of the trigger of centriole biogenesis, PLK4, is required. We used *Xenopus* egg extracts, which allow tight cell-cycle synchrony and are naturally acentriolar, and therefore are uniquely suited to investigate the biochemical

regulation of de novo centriole biogenesis in the absence of physical constraints imposed by the close proximity of the mother centriole. Endogenous *Xenopus* PLK4 (PLX4) is not detectable in extracts and not sufficient to generate MTOCs de novo, presumably due to low expression levels of this kinase [23]. However, overexpression of PLX4 is sufficient to induce de novo assembly of γ -tubulin-containing MTOCs [22], offering an assay to understand the biochemical connection between the cell cycle and PLK4's role in MTOC formation.

PLX4 Can Only Trigger De Novo MTOC Formation after Exit from M Phase

We used the well-characterized cyostatic factor (CSF) extract, which is prepared from *Xenopus* eggs arrested at the second meiotic metaphase (MII) by the CSF. This extract allows the sequential study of three different biochemical states. The first is the CSF-arrested state (Figure 1A) (from here on referred to as "M phase"), which has high CDK1-CyclinB activity. The second is a CSF exit/M exit state, which normally commences

following fertilization but can be artificially induced through the addition of Ca^{2+} to the M phase extract [24]. The addition of Ca^{2+} inactivates the CSF, followed by cyclin degradation by the anaphase-promoting complex (APC/C) and dephosphorylation of CDK1-CyclinB substrates, such as Cdc25 (Figure 1A). This biochemical state corresponds to a very low CDK activity state. Finally, we use an interphase (CSF-released) state, a later time point after Ca^{2+} addition to the CSF extract, which corresponds to S phase, as embryonic cycles are devoid of defined gap phases, such as G1 [25] (Figure 1A).

Addition of recombinant *Xenopus* PLK4 (rPLX4^{WT}) induces de novo assembly of MTOCs in cycling extracts positive for γ -tubulin [22] (Figure S1A) and other centriolar markers (Cep135, Centrin-1) (Figure S1B). Despite the similarity to centriole biogenesis, we never observed 9-fold symmetrical structures by electron microscopy (not shown), suggesting the lack of a limiting assembly factor.

To specifically inhibit PLK4's activity along the cell cycle, we generated an ATP-analog-sensitive recombinant PLX4 variant (also called a "Shokat kinase" [26]), which can be specifically inhibited by ATP analogs. Previously, the substitution of a leucine residue by a glycine (L89G) in the ATP-binding pocket of hsPLK4 was reported to enhance the sensitivity to ATP analogs as desired [27] (Figure S2A), albeit at the cost of a 10-fold reduction in activity in the absence of the ATP-analog inhibitor [27] (Figure S2B). After testing several combinations, we determined that an L89A substitution combined with a compensatory mutation outside of the ATP-binding pocket (H188Y) [28] (Figures S2A and S2B) restored both human and *Xenopus* PLK4 activities to wild-type levels (Figures S2B and S2C). Hereafter, these Shokat alleles of PLK4 are referred to as recombinant analog-sensitive PLX4/PLK4 (rPLX4^{AS}/PLK4^{AS}). Recombinant PLX4^{AS} induced de novo formation of MTOCs as efficiently as rPLX4^{WT} (Figure 1B; Movie S1). The ATP analog 1-naphthyl-PP1 (1-NA-PP1) [29] was found to be a potent inhibitor of rPLX4^{AS} in vitro (Figures S2D and S2E; Movie S2), but not of rPLX4^{WT} (not shown).

Addition of rPLX4^{AS} to either M phase (Figure 1C, i) or M exit extracts (Figure 1C, ii) allowed MTOCs to form after M phase exit. Addition of rPLX4^{AS} in interphase itself (when the extract had completely exited M phase; "CSF-released") did not trigger MTOC formation (Figure 1C, iii). To further investigate the timing, we added rPLX4^{AS} in M phase and inhibited by 1-NA-PP1 in M phase (Figure 1D, iv) at the exit of M phase (Figure 1D, v) or in interphase (Figure 1D, vi). We only observed MTOC formation if rPLX4^{AS} was active at M exit, suggesting that it triggers de novo MTOC formation at a stage in which CDK activity is very low.

Centriole Duplication in Human Cells Requires Active PLK4 after Exit from Mitosis

To investigate whether a similar temporal requirement for PLK4 activity operates in the presence of centrioles and defined G1 and G2 phases, we generated a HeLa cell line conditionally expressing the human Shokat allele PLK4^{AS} (L89A/H188Y) (Figures S2A, S2B, and S2F). Cells were simultaneously depleted of endogenous PLK4 and induced to express RNAi-resistant PLK4^{AS}, which rescued the reduction in centriole number caused by depletion of endogenous wild-type PLK4 (Figure S2G). Importantly, although 1-NA-PP1 treatment alone had no effect on centriole number or cell-cycle progression (not

shown), addition of 1-NA-PP1 to the growth media ablated the ability of PLK4^{AS} to rescue centriole duplication, whereas RNAi-resistant PLK4^{WT} (expressed from the same tetracycline-inducible promoter) was unaffected (Figure S2G).

1-NA-PP1 was added to synchronous cells expressing PLK4^{AS} (and depleted of endogenous PLK4) at mitosis, G1, S, and G2 phases (monitored by flow cytometry and 5-ethynyl-2'-deoxyuridine [EdU] incorporation; Figures 2A and 2B; enlarged in Figures S2H and S2I). The percentage of cells with the expected four centrioles in the subsequent mitosis was assessed. Similar to *Xenopus* extracts, inhibition of PLK4 in a low CDK stage (mitotic exit and G1) reduced the percentage of cells able to duplicate their centrioles by approximately 4-fold (Figures 2A and 2B). Surprisingly, given that centrioles start being assembled in S phase, PLK4 inhibition during S phase or G2 had no major effect on the number of centrioles present in mitotic cells in the same cycle (Figures 2A and 2B). We confirmed these findings using the recently described PLK4-specific inhibitor centrinone [30]. Only cells inhibited from mitosis onward of the previous cycle or from G1 of the same cycle showed a significant decrease in centriole-duplication efficiency (Figure 2C; Figure S2J), suggesting, again, that PLK4 acts in low CDK activity stages. In human cells, we could not perform controlled experiments of inhibition in mitosis followed by release of inhibition, as PLK4 catalyzes its own degradation [3]. Inhibited PLK4 accumulates, causing centriole overamplification upon inhibitor wash-off (previously shown in [30]).

The PLK4-STIL Complex Only Forms upon M Exit

To understand the regulation of PLK4 activity in time, we focused on the first reported event of centriole biogenesis—the formation of the PLK4-STIL complex—and asked whether it occurs at M exit/G1. We first confirmed that STIL has a conserved role in MTOC formation in *Xenopus* extracts (Figures S3A–S3D). STIL is present, and its depletion precluded the formation of rPLX4-induced MTOCs (Figures S3A–S3C). Moreover, rPLX4^{AS} was able to bind and phosphorylate STIL (Figure S3D). Our results suggest a general, conserved mechanism in which STIL is phosphorylated by PLK4 and is required for rPLX4-induced MTOC formation, similar to what is described for human cells [7–10]. Next, we observed that rPLX4 cannot bind STIL in M phase but only after M exit (Figure 3A), at which time it can also phosphorylate it (see shift of STIL band; Figure 3B).

We then asked how PLK4-STIL complex formation is regulated in the presence of centrioles in human cells. We immunoprecipitated FLAG-PLK4 from HeLa cells synchronized in different cell-cycle stages preceding S phase onset: mitosis (M) and early (3 hr post-mitosis [PM]), mid (6 hr PM), and late (9 hr PM) G1 (Figures 3C–3E; Figure S3E). Even though both STIL and PLK4 concentrations are highest in mitosis (Figures 3C–3E; Figures S3F, S4A, and S4B) [15, 16], PLK4-STIL interaction was only observed during mid- and late G1 phases, 6 and 9 hr after mitotic exit, respectively (Figure 3D; Figure S3E). PLK4 is detectable at the centrosome in those stages (Figures S4A and S4B) and, consistently, the percentage of cells with STIL localizing to the centrosome increased significantly starting at mid-G1 (Figure 3E). This was followed by a significant increase of cells with SAS6 localizing to the centrosome in late G1 (9 hr PM; Figure S3G). Importantly, cells treated with the PLK4

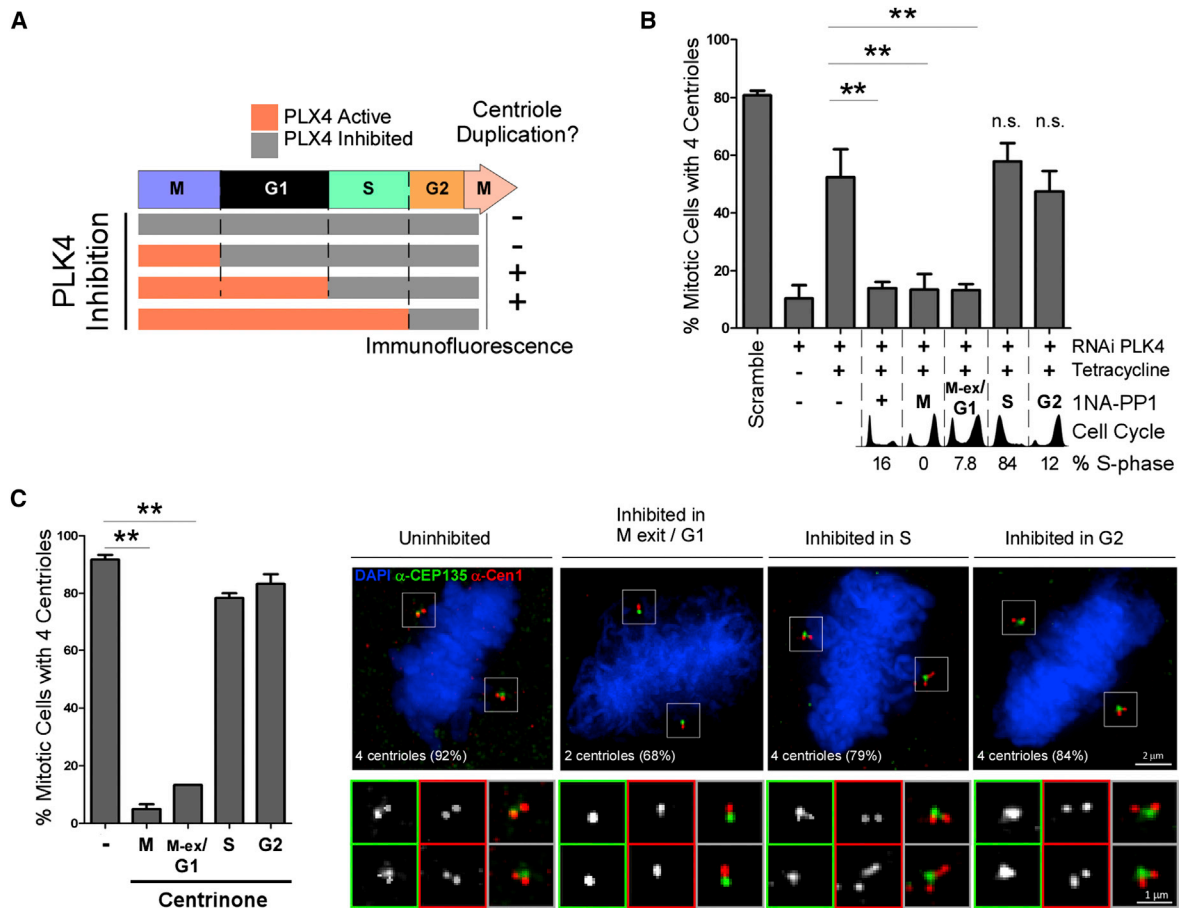


Figure 2. PLK4 Activity Is Needed at M Phase Exit/G1 for Centriole Duplication in Human Cells

PLK4 activity was inhibited at different cell-cycle times by 1-NA-PP1 (PLK4^{AS}) (B) or centrione (C), and centrioles were counted in the subsequent mitosis.

(A) Experimental scheme and summary of results from (B) and (C).

(B) 1-NA-PP1 was added to cells expressing PLK4^{AS} and depleted of endogenous PLK4 at 0 (positive control; +), 6 (G2), 8 (M), 10 (M exit/G1), and 20 hr (S phase) following S phase block release. Cells were fixed in the immediate subsequent mitosis and centrioles were counted (n = 3; 100 cells/condition; mean \pm SEM; **p < 0.01; n.s., not significant). Cell-cycle profiles were obtained by flow cytometry. Percentages of S phase cells at time of inhibition were monitored by EdU staining (see also Figures S2F–S2I for controls).

(C) Centrione was added at the indicated cell-cycle stages and centrioles were counted in the subsequent mitosis (n = 3; 100 cells/condition; mean \pm SEM; **p < 0.01). Representative immunofluorescence images of mitotic cells stained as indicated, following inhibition of PLK4 by centrione. The number of centrioles found with the highest frequency upon inhibition is shown (average of three experiments). See Figure S2J for detailed quantitation.

inhibitor centrione for 1 hr prior to fixation showed a marked reduction in STIL and SAS6 presence at the centrosome in G1, but not in mitosis (Figure 3E; Figure S3G). Our observations suggest that either the recruitment or the maintenance of STIL, and consequently of SAS6, at the centrosome in human cells is dependent on PLK4 activity during G1.

Taken together, our results show that despite the fact that both STIL and PLK4 are present at high CDK1-CyclinB activity states in both acentriolar *Xenopus* egg extracts and in human cells, the two proteins do not form a complex in either of the systems at these stages (Figure 3), suggesting a conserved inhibitory mechanism related to CDK1-CyclinB activity.

Inhibiting CDK1-CyclinB Allows for PLK4-STIL Complex Assembly

We asked whether direct inhibition of CDK1 by the CDK1 inhibitor RO-3306 [31] would permit unscheduled complex for-

mation. CDK1 inhibition in M phase released the extracts to interphase, and this was sufficient for rPLX4 to bind—and likely phosphorylate—STIL (see STIL mobility shift upon rPLX4 addition; Figures 4A and 4B) and to induce MTOC formation (Figure 4C). Likewise, acute inhibition of CDK1 activity in human cells blocked in mitosis restored the PLK4-STIL interaction (Figure 4D; Figure S4C). Taken together, these results strongly corroborate an inhibitory function of CDK1 in PLK4-STIL complex assembly.

CDK1-CyclinB Phosphorylates and Binds to STIL

CDK1-CyclinB prevents the initiation of DNA replication (i.e., licensing) both by phosphorylation of (i.e., Orc2) and binding to (i.e., Orc6) components that are required for this step [32, 33]. We thus asked whether CDK1-CyclinB could regulate PLK4-STIL complex assembly, by phosphorylating and/or binding to STIL.

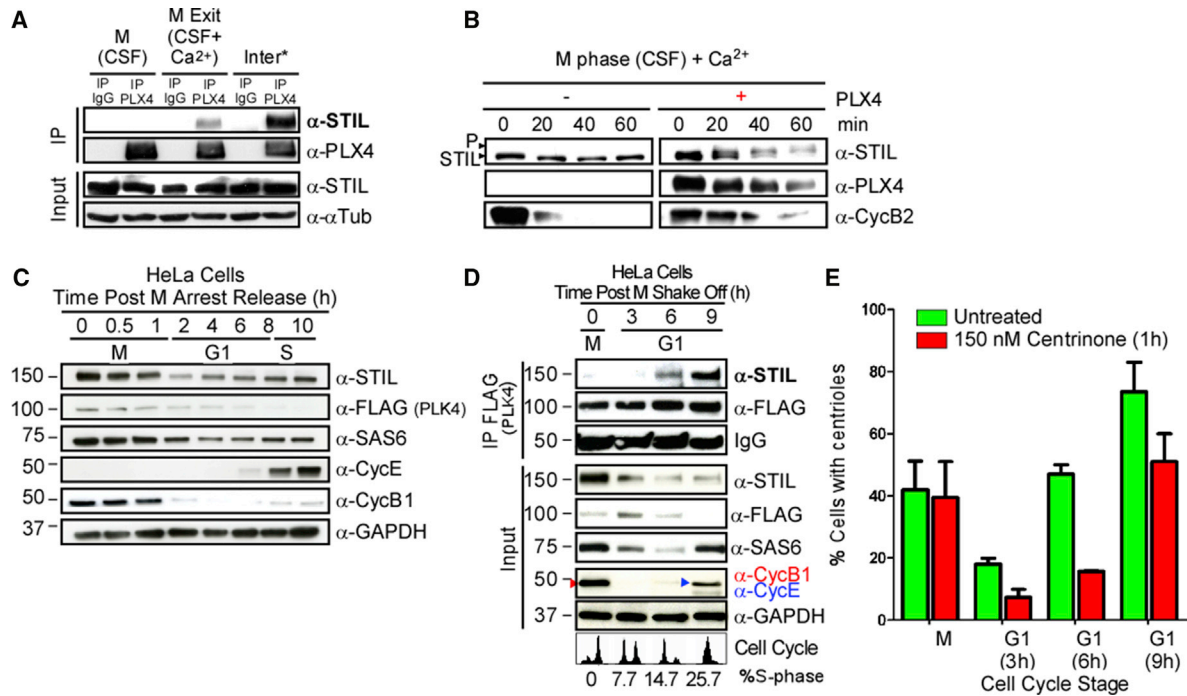


Figure 3. The PLK4-STIL Complex Forms Only upon M Exit in *Xenopus* Extracts and Human Cells

(A) PLX4 binds STIL only after mitotic exit in *Xenopus* extracts (see also Figures S3A–S3D). rPLX4 was added to extracts at the indicated stages and subsequently immunoprecipitated (IP PLX4). Samples were analyzed by WB and probed with the indicated antibodies. The asterisk refers to an interphase extract (see the Experimental Procedures).

(B) PLX4 is likely to phosphorylate STIL upon M exit in *Xenopus* extracts. Released extracts were supplemented with rPLX4. STIL phosphorylation (note the mobility shift) and levels of Cyclin B2 were analyzed by WB.

(C) STIL peaks in mitosis in human cells. FLAG-PLK4-overexpressing HeLa cells were synchronized in mitosis by monastrol and released. Samples were collected at the indicated times.

(D) The PLK4-STIL complex forms in mid-G1. FLAG-PLK4 was immunoprecipitated from cell lysates at the indicated stages. Samples were probed with the indicated antibodies. Cell-cycle profiles were obtained by flow cytometry combined with BrdU-FITC labeling of cells in S phase. See Figure S3E for more details.

(E) STIL recruitment to the centrosome during mid-G1 phase is dependent on PLK4 activity. The presence of STIL at the centrosome was quantified by immunofluorescence using anti-STIL in mitotic or G1 cells obtained after mitotic shake-off. DMSO (control) or centrinone (PLK4 inhibitor) was added 1 hr prior to fixation. The absence of S phase cells in G1 was corroborated by EdU incorporation ($n = 3$; 100 cells/condition; mean \pm SEM). See also Figures S3F, S3G, S4A, and S4B for more details of these experiments.

Given that STIL is highly phosphorylated in M phase (Figure S5A) and its localization at the centrosome is dependent on CDK1 activity [34], we tested whether it is a substrate of CDK1-CyclinB. In vitro kinase assays showed incorporation of ^{32}P -radiolabeled ATP into STIL in the presence of either CDK1-CyclinB or PLX4 (positive control) (Figures S5A and S5B).

We then asked whether CDK1-CyclinB could phosphorylate and/or bind the domains/residues in STIL that normally bind/are phosphorylated by PLK4, to prevent their interaction. PLK4 binds to STIL in the coiled-coil (CC) domain [7–10] (Figure 5A) and phosphorylates STIL on a domain known as the STAN motif, leading to SAS6 recruitment and cartwheel assembly [7–10]. We used hemagglutinin (HA)-tagged full-length STIL (FL) and truncated STIL fragments previously described by Ohta and colleagues [7] (ΔCC , N-terminal domain [N], and N3C; Figure 5A) expressed in HEK293T cells as substrates in an in vitro kinase assay. Importantly, we showed that CDK1-CyclinB phosphorylates the N-terminal domain of STIL but not the region encompassing the CC or STAN motifs (Figures 5B and 5C; confirmed with phospho-specific antibodies against a residue phosphory-

lated by PLK4 S1116 in the STAN domain [8] in Figure 5D). Therefore, CDK1-CyclinB phosphorylates STIL, but on a physically distinct site from the one bound and phosphorylated by PLK4.

We then tested whether CDK1-CyclinB could bind STIL in vivo. We observed that indeed CDK1-CyclinB co-immunoprecipitates with STIL in *Xenopus* extracts arrested in M phase, but not after M exit when Cyclin B is degraded (Figures 6A and 6B). Similarly, when treating M phase extracts with the CDK1 inhibitor RO-3306 in which the CDK1-CyclinB complex is inactive but Cyclin B is not degraded due to the natural absence of Cdh1, inactivated CDK1-CyclinB could not bind STIL (Figure S5C1). Conversely, PLK4 binding to STIL was re-established (Figure S5C2).

We then asked whether binding of CDK1-CyclinB to STIL would prevent STIL from interacting with PLK4. We performed CDK1-CyclinB immunoprecipitation from HEK293T cells expressing HA-tagged FL-STIL or the truncated fragments: ΔCC , which does not bind PLK4 [7–10], and an N-terminal domain. We found that whereas CDK1-CyclinB binds FL-STIL and N-STIL, it does not bind ΔCC -STIL (Figures 6A and 6C). Despite this, ΔCC -STIL is phosphorylated by CDK1-CyclinB

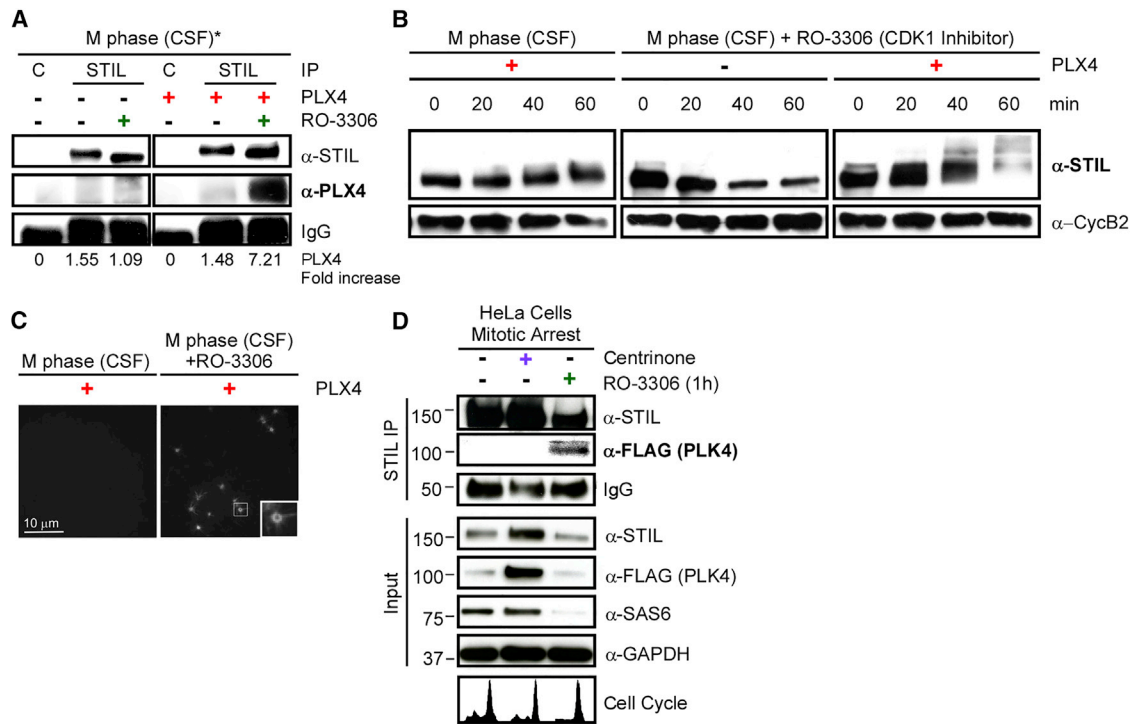


Figure 4. PLK4-STIL Complex Formation Is Inhibited by CDK1

(A) Inhibiting CDK1 allows PLK4-STIL complex assembly. STIL was immunoprecipitated from extracts treated as indicated. Samples were analyzed by WB and probed with the indicated antibodies. Fold increase over control in signal intensity was quantified for each condition. Note that endogenous PLX4 is undetectable. The asterisk indicates the addition of RO-3306, a CDK1 inhibitor, releasing the extract into interphase.

(B) Phosphorylation of STIL in CSF/M phase-arrested extracts treated with RO-3306. M phase extracts were treated as indicated. STIL phosphorylation and Cyclin B2 were analyzed by WB.

(C) PLX4 induces asters in M phase extracts released with RO-3306. Confocal images of M phase extracts supplemented with rPLX4 and 100 μ M RO-3306 in the presence of TRITC-labeled tubulin. Inset represents an enlarged aster of the respective box in the image.

(D) CDK1-CyclinB activity is inhibitory for the formation of the PLK4-STIL complex. Nocodazole-arrested cells in mitosis were treated as indicated. STIL was immunoprecipitated and samples were probed with the indicated antibodies. Note that under centrinone treatment, PLK4 accumulates [30]. Cell-cycle profiles were obtained by flow cytometry; see Figure S4C for details.

(Figure 5B), suggesting that in vitro phosphorylation and binding are not mutually dependent. More importantly, our results show that binding of CDK1-CyclinB to STIL requires the CC domain of STIL.

We then asked whether the CC domain is sufficient for CDK1-CyclinB binding. Immunoprecipitated CDK1 from HEK293T cells expressing GFP-CC [10] or GFP-FL STIL is able to efficiently bind both GFP-CC and GFP-FL (but not GFP alone) (Figure 6D). Our results demonstrate that the CC domain is both necessary and sufficient for CDK1-CyclinB binding to STIL.

CDK1-CyclinB Binds STIL, Preventing STIL-PLK4 Complex Formation and STIL Phosphorylation by PLK4

Our results raise the intriguing possibility that CDK1-CyclinB and PLK4 may compete for binding to STIL. We tested this hypothesis using a glutathione S-transferase (GST)-N3C- Δ STAN-STIL fragment. Remarkably, we observed that although both proteins can interact separately with GST-N3C- Δ STAN (Figure 6E, I and II; Figure S6A), initial incubation of this fragment with CDK1-CyclinB prevents PLX4 from binding to it (Figure 6E, III; Figure S6A). Moreover, this assay was performed in the absence of ATP, reinforcing that binding and phosphorylation of STIL by

CDK1-CyclinB might not be linked. Importantly, we observed that increasing concentrations of CDK1-CyclinB are able to physically displace a constant amount of PLK4 from binding STIL immunoprecipitated from *Xenopus* interphase extracts (Figure S6B).

Finally, we asked whether CDK1-CyclinB-STIL binding would also preclude STIL phosphorylation by PLK4 in the STAN motif, which is the critical event that recruits SAS6 [7, 8, 11]. We used FL-STIL and incubated it with PLK4 and CDK1-CyclinB individually or sequentially, and asked whether PLK4 can phosphorylate STIL in S1116 (Figure 6F). If PLK4 accesses STIL alone, or first, it is able to phosphorylate S1116 (Figure 6F, III). However, pre-incubation of CDK1-CyclinB precludes PLK4 phosphorylation (Figure 6F, IV). Previous reports indicated that PLK4 interaction with STIL enhances PLK4's activity [8]. Consistently, we observed that PLK4 autophosphorylation is reduced when its binding to STIL is disrupted by the presence of CDK1-CyclinB (see ³²P-PLK4 levels in Figure S6C, III versus IV). In summary, we show that CDK1-CyclinB prevents STIL-PLK4 interaction by binding STIL in a kinase-independent fashion through the same region as PLK4. In turn, this prevents both the phosphorylation of STIL by PLK4 and further activation of PLK4. Given the

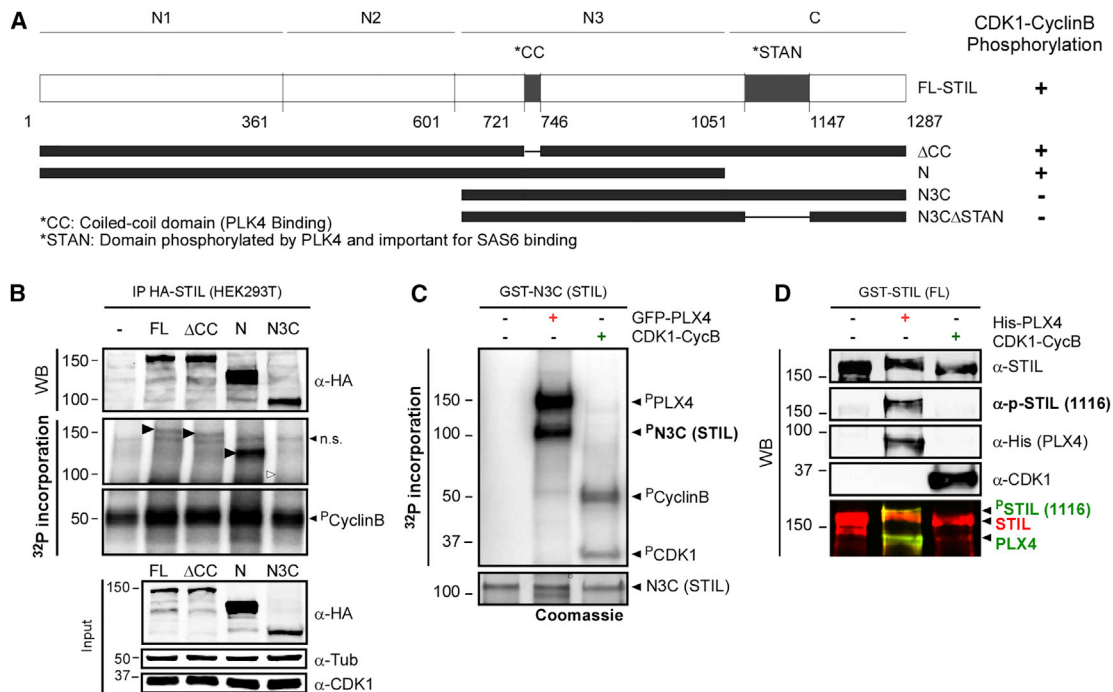


Figure 5. CDK1-CyclinB Phosphorylates STIL outside of the PLK4-Interacting Domain in Human Cells

(A) Schematic representation of HA- and GST-tagged STIL constructs. The evolutionarily conserved coiled-coil (CC; PLK4-binding) and STAN (PLK4-phosphorylated and SAS6-binding) domains are indicated. Constructs were used for phosphorylation assays. The results are summarized on the right.

(B) CDK1-CyclinB can phosphorylate STIL on its N terminus. Autoradiography of an in vitro kinase assay using IP control or HA-STIL (FL, ΔCC, N, and N3C), CDK1-CyclinB, and [γ - 32 P]ATP. Black arrowheads indicate phosphorylated fragments. The white arrowhead indicates the expected position of the non-phosphorylated N3C fragment (n.s., non-specific). Note that all fragments, but not the N3C, are phosphorylated by CDK1-CyclinB.

(C) STIL-N3C, the domain that interacts with PLK4 and SAS6, is not phosphorylated by CDK1-CyclinB. Incorporation of γ - 32 P on STIL-N3C incubated with GFP-PLX4 or CDK1-CyclinB was visualized by autoradiography.

(D) CDK1-CyclinB does not phosphorylate STIL on the site phosphorylated by PLK4 (S1116). Recombinant GST-STIL (FL) was incubated with rPLX4 or CDK1-CyclinB. Samples were analyzed by WB using anti-pS1116-STIL (which recognizes PLK4-specific phosphorylation [8]), anti-His, and anti-CDK1 to monitor loaded proteins.

low concentration of PLK4 in the cell [23], it is likely that CDK1-CyclinB is able to prevent PLK4's binding to STIL in mitosis.

DISCUSSION

A critical ill-understood question in centriole biogenesis is how the cell-division and centriole-duplication cycles are coupled, so that centriole assembly occurs once and only once per cell cycle. Here we show how the first known biochemical event in centriole biogenesis, the association between PLK4 and its substrate STIL, is regulated during the cell cycle. We demonstrate that PLK4 activity is needed for centriole biogenesis before pro-centrioles become detectable in S phase. PLK4 binds and phosphorylates STIL in mid-G1. We show that the major mitotic kinase, CDK1-CyclinB, prevents precocious PLK4-STIL complex assembly and STIL phosphorylation in mitosis by binding to STIL in the same CC domain. These observations strongly support a model in which (1) in S phase and early G2, centriole reduplication is inhibited by centriole physical proximity; (2) in early mitosis, although centrioles overcome the critical distance that prevents reduplication [18–20], and PLK4 and STIL levels are very high [15, 16], CDK1-CyclinB prevents STIL from interacting with and being phosphorylated by PLK4, releasing it

from the centriole [34]; (3) after mitotic exit, following inactivation of CDK1, and new synthesis of STIL and PLK4 in mid-G1, PLK4 can bind and phosphorylate STIL [7–10, 35]; and (4) phosphorylated STIL recruits SAS6 [8, 9, 11] and new cartwheel formation starts at the G1/S boundary [12]. Our work provides a mechanistic link between cell-cycle progression and centrosome biogenesis and a rationale for the observation that centriole biogenesis can only start after exit from mitosis.

Our model is supported by previous unexplained findings: inhibition of CDK1-CyclinB in *Drosophila* wing disc cells, Chinese hamster ovary cells, and chicken DT40 cells leads to unscheduled centriole formation [36, 37]. Moreover, previous work from our laboratory demonstrated that PLK4 overexpression can only drive de novo centriole biogenesis upon exit from meiosis in *Drosophila* eggs, suggesting that inhibition by CDK1-CyclinB in M phase could limit PLK4 activity in many contexts [21]. We note, however, that our model does not exclude additional roles of CDK1 in centriole biogenesis regulation through the activation or inhibition of additional regulators and/or substrates.

Remarkably, the results we present here can be paralleled to licensing mechanisms shown originally to operate in DNA replication and, more recently, centromere assembly (for a review of this topic, see [38]) in certain aspects. In both cases, critical

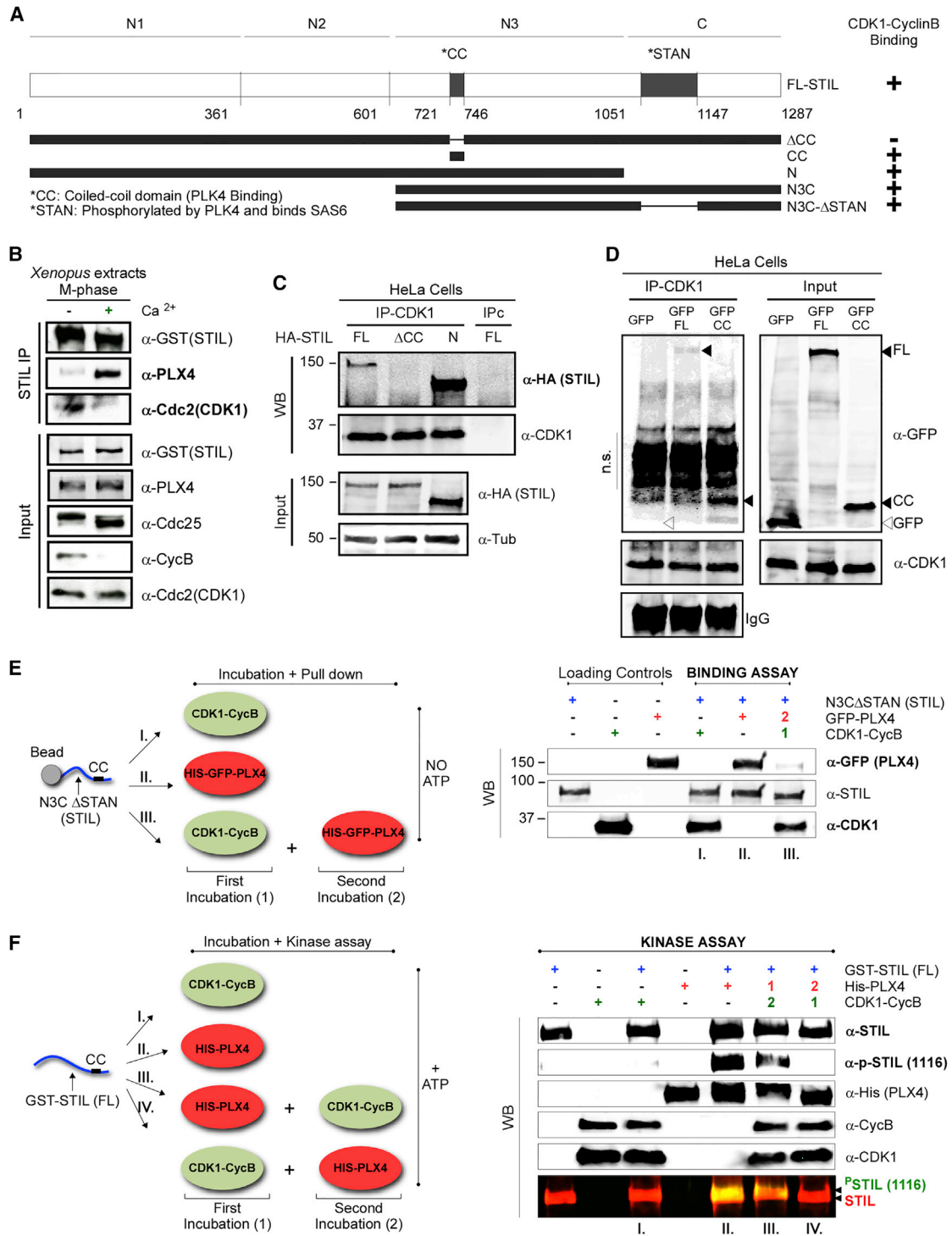


Figure 6. CDK1-CyclinB Binds STIL on Its CC Domain and Competes with PLK4 Binding

(A) Representation of HA-, GST-, and GFP-tagged STIL constructs and summary of results. The evolutionarily conserved CC (PLK4-binding) and STAN (PLK4-phosphorylated and SAS6-binding) domains are indicated.

(B) CDK1-CyclinB and PLK4 bind STIL at different stages. rGST-STIL and rPLX4 were added to CSF extracts, which were kept arrested or released to interphase with Ca^{2+} . GST-STIL was immunoprecipitated and samples were analyzed by WB. See Figures S5C1 and S5C2.

(C) The STIL-CC motif is necessary for CDK1-CyclinB binding. HEK293T cells were transfected with the indicated plasmids and CDK1 was immunoprecipitated. Samples were visualized by WB using the indicated antibodies. IPC, immunoprecipitation control.

(legend continued on next page)

“licensing” events can only occur in G1. This is the loading of the helicase that unwinds the DNA onto the origins of replication, or the loading of the centromeric histone H3, CENP-A, to centromeres. CDK1 inactivates the licensing factor Cdt1 and binds to Orc6 [32, 33, 39], and also prevents loading of CENP-A in different ways [40]. Therefore, both in the case of DNA replication and centromere assembly, CDK1 prevents untimely interactions, ensuring those events occur only once per cell cycle. Assembly of the PLK4-STIL complex in G1, separated from centriole assembly in S phase, can be thought of as a sort of licensing event for centriole duplication, ensuring it occurs “once and only once” per cell cycle. Additional layers of regulation, such as centriole proximity [17, 18], clearly operate in addition to the mechanism we uncovered here to prevent unscheduled licensing in S and G2 phases.

Our results raise several important questions for understanding how centriole numbers are controlled. Whereas binding of CDK1-CyclinB to STIL requires an active CDK1-CyclinB complex, it is not phosphorylation dependent (Figure 6E), giving rise to the intriguing possibility that phosphorylation and binding could regulate independent aspects of STIL’s biology in the cell. Where is CDK1 binding STIL—is it in the cytoplasm or the centrosome pool? Furthermore, how are degradation of STIL by the APC/C in mitotic exit [15, 34] and translation dynamics of new protein pools in G1 fine-tuned? Understanding these will explain why critical events start in mid-G1 and not immediately after Cyclin B degradation. Finally, what role do CDK2-Cyclin complexes [41–45] play in regulating PLK4-STIL complex formation? Quantitative knowledge of the different pools of players, their affinity to each other, and the regulatory mechanisms will lead to a more cohesive understanding of the overarching principles governing the cell-cycle coordination of synchronously occurring cellular processes.

EXPERIMENTAL PROCEDURES

This research project was ethically reviewed and approved by the Ethics Committee of the Instituto Gulbenkian de Ciência (license reference: A007.2010), and by the Portuguese National Entity that regulates the use of laboratory animals (Direção Geral de Alimentação e Veterinária [DGAV]; license reference 0421/000/000/2015). All experiments conducted on animals followed the Portuguese (Decreto-Lei 113/2013) and European (Directive 2010/63/EU) legislations concerning housing, husbandry, and animal welfare.

Plasmids, Cloning, Protein Expression, and Cell Culture

PLX4 and PLX4^{AS} cDNAs were cloned into pFastBac HTb plasmid and expressed in SF21 cells. HeLa cell lines were generated by electroporation of small interfering RNA (siRNA)-resistant cDNA of 3xFLAG-SBP-hPLK4^{AS/WT}. HA-tagged FL-hSTIL, ΔCC, N [7], and GFP-CC [10] were expressed in HEK293T cells. GST-N3C (ΔSTAN) was generated in a previous study [7]. Protein expression was performed as described previously [7].

Protein Detection

Cell lysis was performed in lysis buffer; 50–75 μg of protein was run on a 4%–15% TGX gel (Bio-Rad), transferred onto a nitrocellulose membrane,

and blotted following standard protocols. Antibodies used for protein detection and immunofluorescence assays are specified in the [Supplemental Experimental Procedures](#). Polyclonal anti-PLX4 was generated in this study.

Preparation of *Xenopus* Egg Extracts and MTOC Formation Assay

CSF-arrested and interphase egg extracts were prepared as previously described [46]. Purified PLX4^{AS} was added to 20 μl of CSF extracts at 0.675 μM and released into interphase by calcium addition (20 mM CaCl₂). MTOCs were analyzed by using tetramethylrhodamine B isothiocyanate (TRITC)-labeled porcine tubulin (Cytoskeleton; TL590M, lot 017).

Synchronization, Depletion, Induction, and Inhibition Experiments in HeLa Cells

Depletion of endogenous PLK4 was performed using siRNA oligonucleotides (see table in the [Supplemental Experimental Procedures](#)). Expression of PLK4^{AS/WT} was induced with tetracycline. 1-NA-PP1 was used to inhibit PLK4^{AS}. Thymidine (2 mM; 17 hr; supplemented with 10 μM EdU or BrdU [bromodeoxyuridine]) was used for S phase block; 100 ng/mL (12 hr) nocodazole or 2.5 μM monastrol (14 hr) was used for mitotic block. G1 time points were obtained by mitotic shake-off.

Immunoprecipitation and Kinase Assays

Immunoprecipitated STIL was washed with RIPA buffer, and co-precipitated proteins were separated on a 4%–15% TGX SDS-PAGE gel (Bio-Rad). Kinase reactions were performed in kinase buffer supplemented with ATP-γS and myelin basic protein. Radioactive kinase reactions were performed in the presence of 1 μCi [³²P]ATP (replenishing ATP between kinases in the case of sequential incubations). For phosphorylation assays, GST-hSTIL (FL) [8] or immunoprecipitated STIL was incubated in kinase buffer supplemented with 500 ng of CDK1-CyclinB and/or 500 ng of PLK4. For sequential incubation, GST-N3C (ΔSTAN) was incubated in binding buffer containing 500 ng of CDK1-Cyclin, washed, subsequently incubated with 500 ng of GFP-PLX4, and eluted in Laemmli buffer. Assays were analyzed by Coomassie staining, autoradiography, or western blotting.

For immunoprecipitation from human cells, 1–2 mg of total whole-cell lysate was incubated with protein G coupled to the appropriate antibody, washed, and eluted in Laemmli buffer.

Immunofluorescence Assays, Microscopy, and Flow Cytometry Analysis

Staining with EdU was performed using the Click-iT EdU Alexa Fluor 647 imaging kit (Thermo Fisher Scientific). Propidium iodide or BrdU staining was analyzed on a BD FACScan flow cytometer. Data were plotted and analyzed using FlowJo (Tree Star). Images were collected on a DeltaVision microscope (Applied Precision) using softWoRx (Applied Precision) or a spinning disk CSU-X1 (Yokogawa) confocal scan head coupled to a Nikon Eclipse Ti-E and controlled using MetaMorph 7.5 (Molecular Devices). Prism (version 5.0c; GraphPad) was used for statistical analysis and plotting.

SUPPLEMENTAL INFORMATION

Supplemental Information includes Supplemental Experimental Procedures, six figures, and two movies and can be found with this article online at <http://dx.doi.org/10.1016/j.cub.2016.03.055>.

AUTHOR CONTRIBUTIONS

S.Z. and M.E.F. performed most cellular and biochemical assays; S.Z. performed most *Xenopus* experiments, with the participation of F.L., S.M.G.,

(D) The STIL-CC motif is sufficient for CDK1-CyclinB binding. CDK1 was immunoprecipitated from HEK293T cells expressing GFP, GFP-CC, or GFP-FL-STIL. Co-immunoprecipitates were probed with the indicated antibodies (n.s., non-specific; cross-reaction of the mouse anti-GFP antibody with rabbit IgGs used to immunoprecipitate CDK1).

(E) CDK1 binding to STIL prevents subsequent PLX4 binding. GST-N3CΔSTAN was incubated as indicated in the scheme and pulled down, and its co-precipitated proteins were analyzed by WB. See [Figures S6A](#) and [S6B](#) for quantification (n = 3) and titration experiments.

(F) CDK1 binding of STIL prevents its phosphorylation by PLX4. GST-STIL (FL) was incubated as shown in the scheme. STIL phosphorylation by PLX4 in the STAN motif was analyzed by WB using the indicated antibodies. See [Figure S6C](#) for more details of this experiment.

and P.D.; C.N., D.B., M.L.-F., and S.G. participated in identifying Shokat mutants and creating cell lines; T.M., A.J.H., S.K.-L., M.O., D.K., and T.L. provided reagents; T.L., S.K.-L., and E.K. provided expertise on *Xenopus* work; S.Z., M.E.F., and M.B.-D. devised all experiments; and S.Z., M.E.F., M.L.-F., and M.B.-D. wrote the manuscript. All authors read and discussed the manuscript.

ACKNOWLEDGMENTS

We are thankful to L. Jansen, M. Godinho, and A. Stankovic for discussions and sharing unpublished protocols. We are also grateful to K. Crnkic, F. Ne-delec, D. Needleman, I. Vernos, C. Field, T. Mitchison, T. Stearns, J. Pines, C. Waterman, P. Marco, S. Lens, R. Hengeveld, S. Werner, K. Dores, G. Marteil, Z. Lygerou, J. Loncarek, C. Lopes, J.R.A. Hutchins, K. Oegema, and T. Mayer for sharing reagents and helpful discussions. EMBO YIP and short-term visit programs supported several visits to EMBL. S.Z. is funded by the ERC and FCT (EXPL/BIM-ONC/0830/2013). M.E.F. is funded by EMBO. The M.B.-D. laboratory is supported by IGC, an EMBO installation grant, ERC grant ERC-2010-StG-261344, and FCT grants (FCT Investigator, EXPL/BIM-ONC/0830/2013, and PTDC/SAU-BD/105616/2008).

Received: February 27, 2015

Revised: December 24, 2015

Accepted: March 1, 2016

Published: April 21, 2016

REFERENCES

- Bettencourt-Dias, M., and Glover, D.M. (2007). Centrosome biogenesis and function: centrosomics brings new understanding. *Nat. Rev. Mol. Cell Biol.* **8**, 451–463.
- Khodjakov, A., Rieder, C.L., Sluder, G., Cassels, G., Sibon, O., and Wang, C.-L. (2002). De novo formation of centrosomes in vertebrate cells arrested during S phase. *J. Cell Biol.* **158**, 1171–1181.
- Zitouni, S., Nabais, C., Jana, S.C., Guerrero, A., and Bettencourt-Dias, M. (2014). Polo-like kinases: structural variations lead to multiple functions. *Nat. Rev. Mol. Cell Biol.* **15**, 433–452.
- Bettencourt-Dias, M., Rodrigues-Martins, A., Carpenter, L., Riparbelli, M., Lehmann, L., Gatt, M.K., Carmo, N., Balloux, F., Callaini, G., and Glover, D.M. (2005). SAK/PLK4 is required for centriole duplication and flagella development. *Curr. Biol.* **15**, 2199–2207.
- Habedanck, R., Stierhof, Y.-D., Wilkinson, C.J., and Nigg, E.A. (2005). The Polo kinase Plk4 functions in centriole duplication. *Nat. Cell Biol.* **7**, 1140–1146.
- Kim, T.-S., Park, J.-E., Shukla, A., Choi, S., Murugan, R.N., Lee, J.H., Ahn, M., Rhee, K., Bang, J.K., Kim, B.Y., et al. (2013). Hierarchical recruitment of Plk4 and regulation of centriole biogenesis by two centrosomal scaffolds, Cep192 and Cep152. *Proc. Natl. Acad. Sci. USA* **110**, E4849–E4857.
- Ohta, M., Ashikawa, T., Nozaki, Y., Kozuka-Hata, H., Goto, H., Inagaki, M., Oyama, M., and Kitagawa, D. (2014). Direct interaction of Plk4 with STIL ensures formation of a single procentriole per parental centriole. *Nat. Commun.* **5**, 5267.
- Moyer, T.C., Clutario, K.M., Lambrus, B.G., Daggubati, V., and Holland, A.J. (2015). Binding of STIL to Plk4 activates kinase activity to promote centriole assembly. *J. Cell Biol.* **209**, 863–878.
- Kratz, A.S., Bärenz, F., Richter, K.T., and Hoffmann, I. (2015). Plk4-dependent phosphorylation of STIL is required for centriole duplication. *Biol. Open* **4**, 370–377.
- Arquint, C., Gabryjczyk, A.M., Imseng, S., Böhm, R., Sauer, E., Hiller, S., Nigg, E.A., and Maier, T. (2015). STIL binding to Polo-box 3 of PLK4 regulates centriole duplication. *eLife* **4**, e07888.
- Dzhindzhev, N.S., Tzolovsky, G., Lipinski, Z., Schneider, S., Lattao, R., Fu, J., Debski, J., Dadlez, M., and Glover, D.M. (2014). Plk4 phosphorylates Ana2 to trigger Sas6 recruitment and procentriole formation. *Curr. Biol.* **24**, 2526–2532.
- Gönczy, P. (2012). Towards a molecular architecture of centriole assembly. *Nat. Rev. Mol. Cell Biol.* **13**, 425–435.
- Fu, J., Hagan, I.M., and Glover, D.M. (2015). The centrosome and its duplication cycle. *Cold Spring Harb. Perspect. Biol.* **7**, a015800.
- Leidel, S., Delattre, M., Cerutti, L., Baumer, K., and Gönczy, P. (2005). SAS-6 defines a protein family required for centrosome duplication in *C. elegans* and in human cells. *Nat. Cell Biol.* **7**, 115–125.
- Arquint, C., Sonnen, K.F., Stierhof, Y.-D., and Nigg, E.A. (2012). Cell-cycle-regulated expression of STIL controls centriole number in human cells. *J. Cell Sci.* **125**, 1342–1352.
- Sillibourne, J.E., Tack, F., Vloemans, N., Boeckx, A., Thambirajah, S., Bonnet, P., Ramaekers, F.C.S., Bornens, M., and Grand-Perret, T. (2010). Autophosphorylation of Polo-like kinase 4 and its role in centriole duplication. *Mol. Biol. Cell* **21**, 547–561.
- Tsou, M.-F.B., and Stearns, T. (2006). Mechanism limiting centrosome duplication to once per cell cycle. *Nature* **442**, 947–951.
- Shukla, A., Kong, D., Sharma, M., Magidson, V., and Loncarek, J. (2015). Plk1 relieves centriole block to reduplication by promoting daughter centriole maturation. *Nat. Commun.* **6**, 8077.
- Mazia, D., Harris, P.J., and Bibring, T. (1960). The multiplicity of the mitotic centers and the time-course of their duplication and separation. *J. Biophys. Biochem. Cytol.* **7**, 1–20.
- Sluder, G., and Rieder, C.L. (1985). Centriole number and the reproductive capacity of spindle poles. *J. Cell Biol.* **100**, 887–896.
- Rodrigues-Martins, A., Riparbelli, M., Callaini, G., Glover, D.M., and Bettencourt-Dias, M. (2007). Revisiting the role of the mother centriole in centriole biogenesis. *Science* **316**, 1046–1050.
- Eckerdt, F., Yamamoto, T.M., Lewellyn, A.L., and Maller, J.L. (2011). Identification of a Polo-like kinase 4-dependent pathway for de novo centriole formation. *Curr. Biol.* **21**, 428–432.
- Jakobsen, L., Vanselow, K., Skogs, M., Toyoda, Y., Lundberg, E., Poser, I., Falkenby, L.G., Bennetzen, M., Westendorf, J., Nigg, E.A., et al. (2011). Novel asymmetrically localizing components of human centrosomes identified by complementary proteomics methods. *EMBO J.* **30**, 1520–1535.
- Desai, A., Murray, A., Mitchison, T.J., and Walczak, C.E. (1999). The use of *Xenopus* egg extracts to study mitotic spindle assembly and function in vitro. *Methods Cell Biol.* **61**, 385–412.
- Tokmakov, A.A., Iwasaki, T., Sato, K., and Fukami, Y. (2010). Analysis of signal transduction in cell-free extracts and rafts of *Xenopus* eggs. *Methods* **51**, 177–182.
- Bishop, A.C., Ubersax, J.A., Petsch, D.T., Matheos, D.P., Gray, N.S., Blethrow, J., Shimizu, E., Tsien, J.Z., Schultz, P.G., Rose, M.D., et al. (2000). A chemical switch for inhibitor-sensitive alleles of any protein kinase. *Nature* **407**, 395–401.
- Holland, A.J., Lan, W., Niessen, S., Hoover, H., and Cleveland, D.W. (2010). Polo-like kinase 4 kinase activity limits centrosome overduplication by autoregulating its own stability. *J. Cell Biol.* **188**, 191–198.
- Hengeveld, R.C.C., Hertz, N.T., Vromans, M.J.M., Zhang, C., Burlingame, A.L., Shokat, K.M., and Lens, S.M.A. (2012). Development of a chemical genetic approach for human Aurora B kinase identifies novel substrates of the chromosomal passenger complex. *Mol. Cell. Proteomics* **11**, 47–59.
- Bishop, A.C., Shah, K., Liu, Y., Witucki, L., Kung, C., and Shokat, K.M. (1998). Design of allele-specific inhibitors to probe protein kinase signaling. *Curr. Biol.* **8**, 257–266.
- Wong, Y.L., Anzola, J.V., Davis, R.L., Yoon, M., Motamedi, A., Kroll, A., Seo, C.P., Hsia, J.E., Kim, S.K., Mitchell, J.W., et al. (2015). Reversible centriole depletion with an inhibitor of Polo-like kinase 4. *Science* **348**, 1155–1160.
- Vassilev, L.T. (2006). Cell cycle synchronization at the G2/M phase border by reversible inhibition of CDK1. *Cell Cycle* **5**, 2555–2556.
- Nguyen, V.Q., Co, C., and Li, J.J. (2001). Cyclin-dependent kinases prevent DNA re-replication through multiple mechanisms. *Nature* **411**, 1068–1073.
- Chen, S., and Bell, S.P. (2011). CDK prevents Mcm2-7 helicase loading by inhibiting Cdt1 interaction with Orc6. *Genes Dev.* **25**, 363–372.

34. Arquint, C., and Nigg, E.A. (2014). STIL microcephaly mutations interfere with APC/C-mediated degradation and cause centriole amplification. *Curr. Biol.* *24*, 351–360.
35. Dzhinzhev, N.S., Yu, Q.D., Weiskopf, K., Tzolovsky, G., Cunha-Ferreira, I., Riparbelli, M., Rodrigues-Martins, A., Bettencourt-Dias, M., Callaini, G., and Glover, D.M. (2010). Asterless is a scaffold for the onset of centriole assembly. *Nature* *467*, 714–718.
36. Vidwans, S.J., Wong, M.L., and O'Farrell, P.H. (2003). Anomalous centriole configurations are detected in *Drosophila* wing disc cells upon Cdk1 inactivation. *J. Cell Sci.* *116*, 137–143.
37. Steere, N., Wagner, M., Beishir, S., Smith, E., Breslin, L., Morrison, C.G., Hohegger, H., and Kuriyama, R. (2011). Centrosome amplification in CHO and DT40 cells by inactivation of cyclin-dependent kinases. *Cytoskeleton (Hoboken)* *68*, 446–458.
38. McIntosh, D., and Blow, J.J. (2012). Dormant origins, the licensing checkpoint, and the response to replicative stresses. *Cold Spring Harb. Perspect. Biol.* *4*, a012955.
39. Enserink, J.M., and Kolodner, R.D. (2010). An overview of Cdk1-controlled targets and processes. *Cell Div.* *5*, 11.
40. Silva, M.C.C., Bodor, D.L., Stellfox, M.E., Martins, N.M.C., Hohegger, H., Foltz, D.R., and Jansen, L.E.T. (2012). Cdk activity couples epigenetic centromere inheritance to cell cycle progression. *Dev. Cell* *22*, 52–63.
41. Kodani, A., Yu, T.W., Johnson, J.R., Jayaraman, D., Johnson, T.L., Al-Gazali, L., Sztriha, L., Partlow, J.N., Kim, H., Krup, A.L., et al. (2015). Centriolar satellites assemble centrosomal microcephaly proteins to recruit CDK2 and promote centriole duplication. *eLife* *4*, e07519.
42. Koff, A., Giordano, A., Desai, D., Yamashita, K., Harper, J.W., Elledge, S., Nishimoto, T., Morgan, D.O., Franza, B.R., and Roberts, J.M. (1992). Formation and activation of a cyclin E-cdk2 complex during the G1 phase of the human cell cycle. *Science* *257*, 1689–1694.
43. Meraldi, P., Lukas, J., Fry, A.M., Bartek, J., and Nigg, E.A. (1999). Centrosome duplication in mammalian somatic cells requires E2F and Cdk2-cyclin A. *Nat. Cell Biol.* *1*, 88–93.
44. Hinchcliffe, E.H., Li, C., Thompson, E.A., Maller, J.L., and Sluder, G. (1999). Requirement of Cdk2-cyclin E activity for repeated centrosome reproduction in *Xenopus* egg extracts. *Science* *283*, 851–854.
45. Matsumoto, Y., Hayashi, K., and Nishida, E. (1999). Cyclin-dependent kinase 2 (Cdk2) is required for centrosome duplication in mammalian cells. *Curr. Biol.* *9*, 429–432.
46. Lorca, T., Bernis, C., Vigneron, S., Burgess, A., Brioudes, E., Labbé, J.-C., and Castro, A. (2010). Constant regulation of both the MPF amplification loop and the Greatwall-PP2A pathway is required for metaphase II arrest and correct entry into the first embryonic cell cycle. *J. Cell Sci.* *123*, 2281–2291.